Selective Recognition of Ammonium over Potassium Ion with Acyclic Receptor Molecules Bearing 3,4,5-Trialkylpyrazolyl Groups

Felix Fuhrmann[a]
Wilhelm Seichter[a]
Monika Mazik*[a]

[a] Institut für Organische Chemie, Technische Universität Bergakademie Freiberg, Leipziger Strasse 29, 09599 Freiberg, Germany
* monika.mazik@chemie.tu-freiberg.de

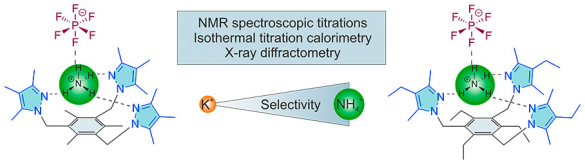

Received: 08.06.2022
Accepted after revision: 06.07.2022
DOI: 10.1055/a-1896-6890; Art ID: OM-2022-06-0007-OA

Abstract Among the 1,3,5-trisubstituted 2,4,6-triethylbenzenes bearing pyrazolyl groups, the compounds with 3,5-dimethylpyrazolyl moieties were found to be effective receptors for ammonium ions (NH_4^+). The current study investigated the extent to which the incorporation of an additional alkyl group in the 4-position of the pyrazole ring affects the binding properties of the new compounds. ^{1}H NMR spectroscopic titrations and investigations using isothermal titration calorimetry revealed that this small structural variation leads to a significant increase in the binding strength towards NH_4^+ and also improves the binding preference for NH_4^+ over K^+. In addition to the studies in solution, crystalline complexes of the new triethyl- and trimethylbenzene derivatives, bearing 3,4,5-trialkylpyrazolyl groups, with $NH_4^+PF_6^-$ were obtained and analyzed in detail. It is noteworthy that two of the crystal structures discussed in this work are characterized by the presence of two types of ammonium complexes. Studies focusing on the development of new artificial ammonium receptors are motivated, among other things, by the need for more selective ammonium sensors than those based on the natural ionophore nonactin.

Key words: molecular recognition, ammonium receptors, selectivity, structure–binding activity relationships

Introduction

The development of new organic molecules suitable for the construction of effective sensor systems, which can selectively recognize ammonium ions (NH_4^+) over other ions, is of great research interest. Selective detection of NH_4^+ is needed to answer various environmental[1a–f] and medical[2a–f] questions, but due to the similarity of ammonium and potassium ions, the realization of this goal represents a challenge. For example, the ionic radii of the ammonium ion (r = 1.40 Å, coordination number, CN = 4)[3a] and the potassium ion (r = 1.38 Å, CN = 6)[3b] differ only slightly.

Most of the sensors used today are based on the natural ionophore nonactin (Figure 1a); however, its binding preference for NH_4^+ over K^+ is not as pronounced as necessary,[4a,b] so alternatives are being sought.[5a]

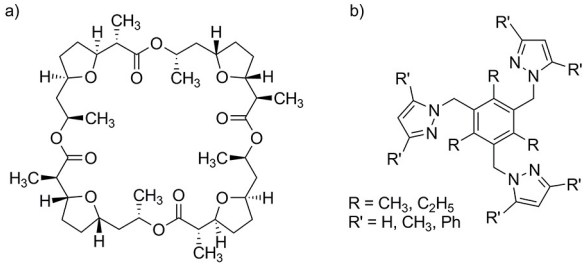

Figure 1 Structure of the natural ionophore nonactin (a) and examples of tripodal benzene derivatives bearing pyrazolyl groups (b).

In the development of artificial receptors, both macrocyclic[5a–g] and acyclic compounds[4a,6,7a–j,8a,b] were considered. Among the acyclic compounds, tripodal[7a–e] and hexapodal[8a,b] benzene derivatives with pyrazolyl or indazolyl groups, for example, were examined (Figure 1b). The ability of these compounds to act as ammonium receptors was investigated both in solution and in the crystalline state[7a–e,8a] (for examples of crystalline ammonium complexes, see Figure 2).

Studies with pyrazole-containing molecules yielded promising results and showed that the substitution pattern of the pyrazole ring has a significant influence on the binding properties of the tested compounds. 1,3,5-Trisubstituted 2,4,6-triethylbenzenes bearing 3,5-dimethylpyrazolyl groups proved to be particularly promising receptors for NH_4^+.[7a–d] The improved NH_4^+/K^+ selectivity of these compounds compared to analogues with unsubstituted pyrazolyl moieties was mainly attributed to the presence of the three pyrazole 3-CH_3 substituents,[7b] which prevent the formation of 2 : 1 receptor–substrate complexes with K^+ and thereby the coordination of this cation. By replacing the methyl groups in positions 3 and 5 of the pyrazole ring with

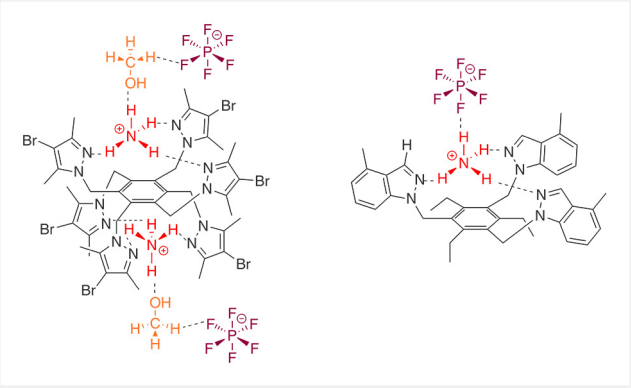

Figure 2 Schematic representations of noncovalent interactions in the crystal structures of two exemplary complexes of hexapodal and tripodal benzene derivatives with NH_4PF_6: complexes of hexakis[(4-bromo-3,5-dimethyl-1*H*-pyrazol-1-yl)methyl]benzene (left)[8a] and of 1,3,5-tris[(4-methyl-1*H*-indazol-1-yl)methyl]-2,4,6-triethylbenzene (right).[9]

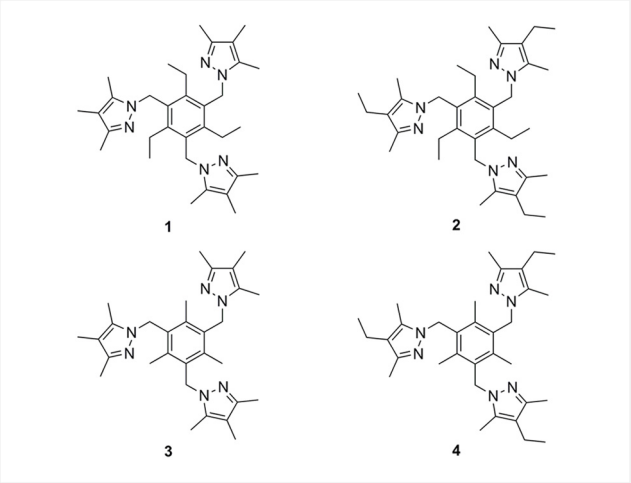

Figure 3 Structures of the new 1,3,5-trisubstituted 2,4,6-triethylbenzene or 2,4,6-trimethylbenzene derivatives bearing 4-alkyl-3,5-dimethylpyrazolyl groups.

phenyl groups, a significant decrease in the binding affinity was observed.[7e] Given the interesting properties of the tripodal benzene derivatives bearing 3,5-dimethylpyrazolyl groups, the current studies investigated the extent to which the incorporation of an additional alkyl group in the 4-position of the pyrazole ring affects the binding properties of the triethyl- and trimethylbenzene derivatives **1–4** towards NH_4^+ (Figure 3).

^{1}H NMR spectroscopic titrations and investigations by isothermal titration calorimetry (ITC) revealed a significant increase in the binding affinity of compounds **1–4**, bearing 3,4,5-trimethyl or 4-ethyl-3,5-dimethylpyrazolyl groups, compared to the analogues containing 3,5-dimethylpyrazolyl moieties. Particularly noteworthy is the excellent NH_4^+/K^+ binding preference of the tested compounds. Crystal structures of the ammonium complexes formed by compounds **1–4** provide valuable information about the interactions that are responsible for the stabilization of the crystalline complexes.

Results and Discussion

Synthesis of compounds 1–4 and their analogues 5 and 6

Compounds **1–4** were prepared through the reaction of 1,3,5-tris(bromomethyl)-2,4,6-triethylbenzene (**7**) or 1,3,5-tris(bromomethyl)-2,4,6-trimethylbenzene (**8**) with the corresponding pyrazole derivative, such as 3,4,5-trimethyl-1*H*-pyrazole (**9**) and 4-ethyl-3,5-dimethyl-1*H*-pyrazole (**10**), as shown in Scheme 1. In addition to the target compounds **1–4**, derivatives **5** and **6** (Scheme 1) have been synthesized in order to compare the binding properties of the new compounds containing 3,4,5-trialkylpyrazolyl groups with those of the known compounds bearing 3,5-dimethylpyrazolyl moieties.

All reactions were carried out under a nitrogen atmosphere, at room temperature, in dry acetonitrile, and in the presence of sodium hydride as a base. The progress of the reactions was monitored by thin layer chromatography (see Experimental Section).

The pyrazoles **9** and **10** were prepared by the reaction of 3-methylpentan-2,4-dione or 3-ethylpentan-2,4-dione with hydrazine monohydrate in methanol (see Scheme 1). The by-product 3,5-dimethyl-1*H*-pyrazole (**11**), which could

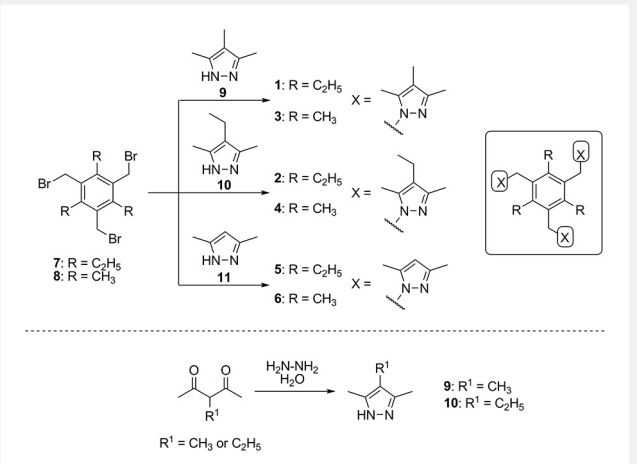

Scheme 1 Reaction conditions for the synthesis of compounds **1–6:** NaH, CH_3CN, N_2 atmosphere (63% of **1**, 65% of **2**, 72% of **3**, 76% of **4**, 87% of **5**, 63% of **6**). Reaction conditions for the preparation of **9** and **10:** 3-methylpentan-2,4-dione or 3-ethylpentan-2,4-dione, hydrazine monohydrate, CH_3OH, 0 °C and then reflux (90% of **9**, 78% of **10**).

not be completely removed by distillation, for example, was successfully separated by taking advantage of the relatively small differences in the NH acidity between pyrazole derivatives **9**–**11**. In this procedure, a dichloromethane solution of the crude reaction product was treated with a NaOH solution (2–5%), resulting in the removal of **11**.

The pyrazole **11** used for the synthesis of compounds **5** and **6** was purchased commercially.

Binding studies: ^{1}H NMR spectroscopic titrations and microcalorimetric titrations

The ability of the compounds **1**–**4** to act as ammonium receptors was evaluated on the basis of ^{1}H NMR titrations and ITC.

The ^{1}H NMR titrations of **1**–**4** with ammonium hexafluorophosphate (NH_4PF_6) and potassium hexafluorophosphate (KPF_6) were performed in CD_3CN or a $CD_3CN/CDCl_3$ mixture at a constant concentration of the receptor. Examples of the complexation-induced shifts observed for compounds **1**–**4** during the titration with NH_4PF_6 and KPF_6 are given in Figures 4 and 5 as well as in the Supporting Information (Figures S2–S7 and Tables S1–S2).

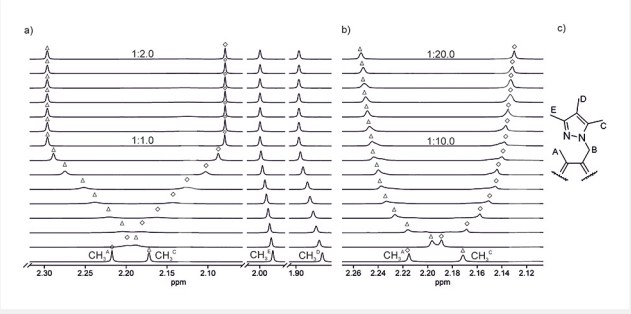

Figure 4 Partial ^{1}H NMR spectra (500 MHz, $CD_3CN/CDCl_3$ 2:1, v/v, 298 K) of compound **3** after the addition of (a) 0.00–2.05 equiv of NH_4PF_6 ([**3**] = 2.53 mM) and (b) 0.00–20.09 equiv of KPF_6 ([**3**] = 2.50 mM). Shown are the chemical shifts of the CH_3^A (marked by diamonds), CH_3^C (marked by triangles), CH_3^D and CH_3^E signals of **3**, for labeling, see (c).

This type of compounds can interact with NH_4^+ via three charge-enhanced NH···N hydrogen bonds involving the nitrogen atom N2 of each of the three pyrazole units. In all cases, the complexation-induced shift of the pyrazole 5-CH_3 signal indicates that the heterocyclic ring undergoes a rotation during the complexation process to ensure binding of the NH_4^+ by the nitrogen atom N2 (see also 2D NMR experiments, Figures S26 and S27 in the Supporting Information).

The titration data were evaluated on the basis of WinEQNMR[10] and SupraFit[11] programs, and the complex stoichiometry was analyzed by using the mole ratio

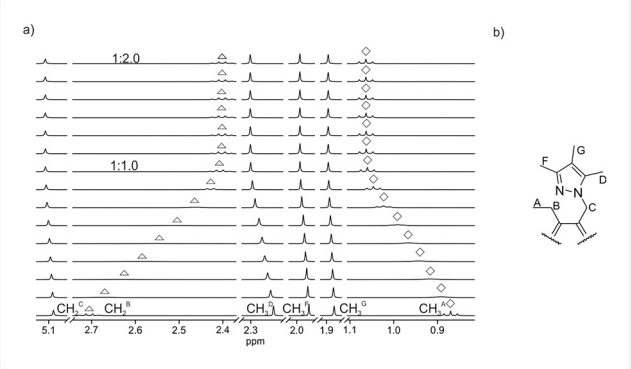

Figure 5 Partial ^{1}H NMR spectra (500 MHz, CD_3CN, 298 K) of compound **1** after the addition of (a) 0.00–2.02 equiv of NH_4PF_6 ([**1**] = 2.51 mM). Shown are the chemical shifts of the CH_3^A (marked by diamonds), $CH_3^{D,F,G}$, CH_2^B (marked by triangles) and CH_2^C signals of **1**, for labeling, see (b).

method.[12] The NMR experiments in $CD_3CN/CDCl_3$ (2:1, v/v) revealed that compounds **1**–**4** form very strong 1:1 complexes with the ammonium ion under the chosen experimental conditions ($K_{11} > 10^5 \cdot M^{-1}$). In contrast, only a weak binding of the potassium ion could be detected ($K_{11} \sim 10^2 \cdot M^{-1}$).

^{1}H NMR titrations of compounds **1** and **2** with NH_4PF_6 were also performed in CD_3CN and showed very strong binding as well, but weaker than in the solvent mixture, as expected. Due to the very strong binding of the ammonium ion, the NMR method could not be used for the exact determination of the binding constants, but this was realised by using the ITC method. The determined association constants are summarized in Table 1.

The microcalorimetric titrations were carried out by adding increasing amounts of the ammonium hexafluorophosphate to a solution of the corresponding receptor in a mixture of dry $CH_3CN/CHCl_3$ (compounds **1**–**6**) or in CH_3CN (compounds **1** and **2**). An example is given in Figure 6 and further examples can be found in the Supporting Information (Figures S11–S17). The binding constants were determined from three independent microcalorimetric titrations and in all cases the best fit of the titration data was obtained with the 1:1 receptor–ammonium binding model (data were evaluated on the basis of NanoAnalyze and SupraFit programs; see Table 2).

The results of the binding studies showed a significant influence of the additional alkyl group at the 4-position of the pyrazole ring on the binding strength of the tested compounds **1**–**4**. In comparison to the analogues bearing 3,5-dimethylpyrazolyl groups, a two- to almost three-fold increase in binding affinity could be observed under the chosen experimental conditions. Although both the presence of an additional methyl substituent and the presence of an ethyl substituent increase the receptor efficiency, the former

Table 1 Association constants[a,b] for the complexation of ammonium hexafluorophosphate (NH_4PF_6) and potassium hexafluorophosphate (KPF_6) with compounds **1–6** (for further details, see Table 2)

Compound	Trialkylbenzene/substituents in the pyrazole ring	K_{11}[c] [M^{-1}] ITC[d]	K_{11}[c] [M^{-1}] NMR[e]
Acetonitrile/chloroform 2:1 (v/v)			
		NH_4PF_6	KPF_6
1	Triethylbenzene/3,4,5-trimethyl	1 280 000	119
2	Triethylbenzene/4-ethyl-3,5-dimethyl	1 150 000	89
5	Triethylbenzene/3,5-dimethyl	451 000	135
3	Trimethylbenzene/3,4,5-trimethyl	752 000	117
4	Trimethylbenzene/4-ethyl-3,5-dimethyl	678 000	105
6	Trimethylbenzene/3,5-dimethyl	326 000	123
Acetonitrile			
1	Triethylbenzene/3,4,5-trimethyl	221 000[c]	–[f]
2	Triethylbenzene/4-ethyl-3,5-dimethyl	152 000[c]	–[f]

[a]Average K_{11} values from multiple titrations: ^{1}H NMR spectroscopic titrations [$CD_3CN/CDCl_3$ (2:1, v/v) or CD_3CN, 298 K; evaluated on the basis of WinEQNMR[10] and SupraFit[11] programs] or microcalorimetric titrations [$CH_3CN/CHCl_3$ (2:1, v/v) or CH_3CN, 298 K; evaluated on the basis of NanoAnalyze and SupraFit programs]. [b]Errors were estimated at < 10%. [c]1:1 Receptor–substrate binding model. [d]Determined by using ITC; the binding constants were too large to be accurately determined by the NMR method. [e]Determined by the NMR method. [f]Not determined.

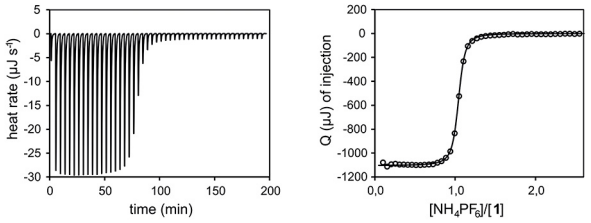

Figure 6 ITC thermogram (left) and titration curve-fitting (right) for the titration of **1** with NH_4PF_6 in dry $CH_3CN/CHCl_3$ 2:1 (v/v) (the heat of dilution has been subtracted). Titration mode: addition of NH_4PF_6 ($c_{syringe}$ = 5.9 mM) into **1** (c_{cell} = 0.5 mM) at 298 K in 46 steps, calorimeter: *MicroCal™ VP-ITC*.

leads to a somewhat stronger increase in binding strength for electronic[13a] and steric[13b,c] reasons. According to the molecular modelling calculations of the free receptors, the pyrazole 4-ethyl groups cause a stronger shielding of the receptor cavity than the 4-methyl substituents, which may also affect the binding process of the substrate.

In agreement with previous studies,[7a,b,e] the strong solvent effects were also observed for the new representatives of this class of compounds. The use of acetonitrile instead of an acetonitrile/chloroform mixture (2:1, v/v) resulted in a six- to seven-fold decrease in the binding strength of the tested receptor molecules towards ammonium hexafluorophosphate.

Table 2 Results of microcalorimetric titrations of compounds **1–6** with ammonium hexafluorophosphate[a–c]

Compound	lg K_{11} (K_{11} [M^{-1}])	ΔG [kJ/mol]	ΔH [kJ/mol]	TΔS [kJ/mol]	ΔS [J/mol K]
Acetonitrile/chloroform 2:1 (v/v)[a]					
1	6.11 ± 0.01 (1 280 000 ± 7700)	−34.86 ± 0.01	−30.3 ± 0.2	4.6 ± 0.2	15.5 ± 0.5
2	6.06 ± 0.01 (1 150 000 ± 1900)	−34.59 ± 0.01	−28.0 ± 0.4	6.6 ± 0.4	22.3 ± 1.2
5	5.65 ± 0.01 (451 000 ± 10 000)	−32.28 ± 0.06	−28.6 ± 0.2	3.7 ± 0.3	12.4 ± 0.9
3	5.88 ± 0.01 (752 000 ± 5900)	−33.54 ± 0.02	−33.0 ± 0.2	0.6 ± 0.2	1.9 ± 0.7
4	5.83 ± 0.03 (678 000 ± 48 000)	−33.28 ± 0.18	−31.7 ± 0.5	1.6 ± 0.4	5.3 ± 1.2
6	5.51 ± 0.02 (326 000 ± 11 000)	−31.47 ± 0.08	−32.5 ± 0.5	−1.0 ± 0.4	−3.5 ± 1.5
Acetonitrile[b]					
1	5.34 ± 0.03 (221 000 ± 17 300)	−30.50 ± 0.19	−26.4 ± 0.1	4.1 ± 0.1	13.9 ± 0.4
2	5.18 ± 0.02 (152 000 ± 8700)	−29.58 ± 0.14	−24.6 ± 0.4	5.0 ± 0.4	16.6 ± 1.4

[a]In dry $CH_3CN/CHCl_3$ 2:1 (v/v) at 25 °C. Used concentrations: [receptor] = 0.5 mM, [NH_4PF_6] = 5.9 mM (calorimeter: *MicroCal™ VP-ITC*); [receptor] = 2.5 mM, [NH_4PF_6] = 18.2 mM (calorimeter: *Thermal Activity Monitor 2277*). [b]In dry CH_3CN at 25 °C. [c]The errors listed are the standard deviations for a minimum of three replicated ITC titrations.

Triethylbenzene-based compounds are more effective receptors for the ammonium ion than their trimethylbenzene-based analogues, as shown by comparing the binding properties of compounds **1, 2**, and **5** with those of **3, 4**, and **6**, respectively (see Tables 1 and 2 and Figure 7). Among the tested compounds, compound **1** was identified as the most powerful ammonium receptor.

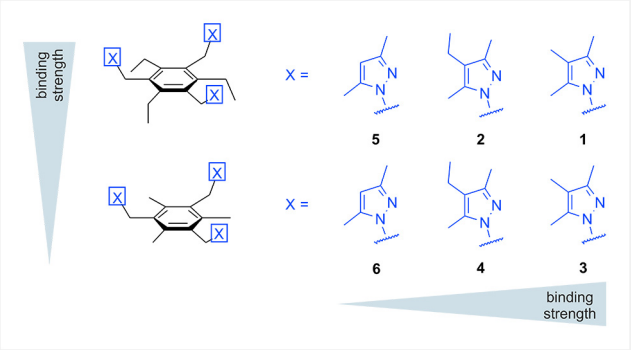

Figure 7 Schematic illustration of how the binding efficiency of the investigated compounds is affected by the substituent at 4-position of the pyrazole ring (considered is the binding strength to ammonium hexafluorophosphate). The higher affinity of the triethylbenzene derivatives in comparison to their trimethylbenzene-based analogues is also schematically illustrated in this figure.

Consideration of the results of the binding experiments revealed that the incorporation of an additional alkyl group into the 3,5-dimethylpyrazole unit resulted in a gain in binding free energy of about 2 kJ/mol.

It is particularly noteworthy that all compounds exhibit excellent binding preference for the ammonium ion compared to the potassium ion. Compounds consisting of triethylbenzene scaffold and 3,4,5-trialkylpyrazole units (compounds **1** and **2**) were found to have the best ability to discriminate between the two ions.

As mentioned above, the complexation of the ammonium ion occurs mainly by NH···N hydrogen bonds (as shown by previous and current binding studies). This is also indicated by molecular modelling calculations (Figure 8) and confirmed by the results of crystallographic studies (see below).

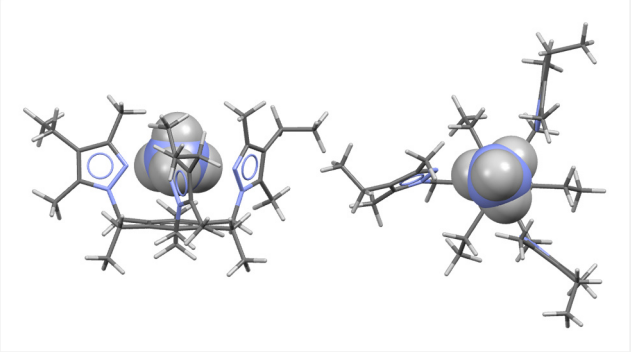

Figure 8 Energy-minimized structure of the 1:1 complex **2**•NH_4PF_6 (two different views; the ammonium ion is located in the cavity of compound **2**). MacroModel V.11.0, OPLS_2001 force field, MCMM, 50 000 steps; color code: H, white; C, grey; N, blue.

Crystal structures of the receptor molecules 1 and 3 and of the ammonium complexes 1a–4a

In the course of our experimental work we succeeded to grow crystalline ammonium complexes of compounds **1**–**4**. They comprise the complexes **1**•$NH_4^+PF_6^-$ (1:1) (**1a**), **2**•$NH_4^+PF_6^-$ (2:2) (**2a**), **3**•$NH_4^+PF_6^-$•HOC_2H_4OH (1:1:0.5) (**3a**), and **4**•$NH_4^+PF_6^-$•C_2H_5OH (2:2:2) (**4a**) (see Figure 9). Moreover, crystallization of the receptors **1** and **3** yielded guest-free crystal structures. The crystals of the complexes were obtained by slow evaporation of the solvent from an ethanol or ethane-1,2-diol solution of a 1:5 mixture of the respective compound and $NH_4^+PF_6^-$, whereas the crystals of **1** and **3** were obtained from hexane and methanol, respectively. Crystallographic data, experimental parameters and selected details of the refinement calculations are summarized in Table S3. The conformation of the receptor (host) molecule can be described by a set of dihedral angles formed by their aromatic building blocks. Their values together with selected torsion angles are listed in Table S4, while informa-

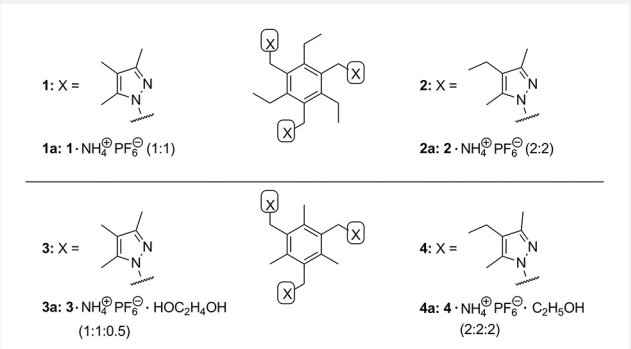

Figure 9 Structures of compounds **1–4** and the composition of the molecular crystals of the complexes **1a–4a**.

tion regarding intermolecular interactions in the crystals is summarized in Table S5.

The crystal structures of **1a**–**4a** are composed of the same kind of receptor–NH_4^+ units in which the NH_4^+ ion resides in a cavity created by the functionalized arms of the receptor molecule. The interaction of the cation with the receptor always involves the nitrogen atoms of the pyrazole units, designated as N(2), N(4) and N(6) in the figures showing the molecular structures.

Triethylbenzene-based compounds: Crystal structures of 1 and complexes 1a and 2a

Compound **1** crystallizes from hexane as colorless rods of the space group *P*-1 with two molecules in the unit cell. Two of the three 3,4,5-trimethylpyrazolyl moieties are directed to one side of the central benzene ring, while the third points in the opposite direction (*aab* arrangement). Taking the ethyl groups into account, the spatial arrangement of the substituents along the periphery of the benzene ring represents an *ab'aa'bb'* pattern (*a* = above, *b* = below, *a'*/*b'* = ethyl; for details, see refs. 7c and 14),[7c,14] as shown in Figures 10a and 11a. The molecular conformation appears to

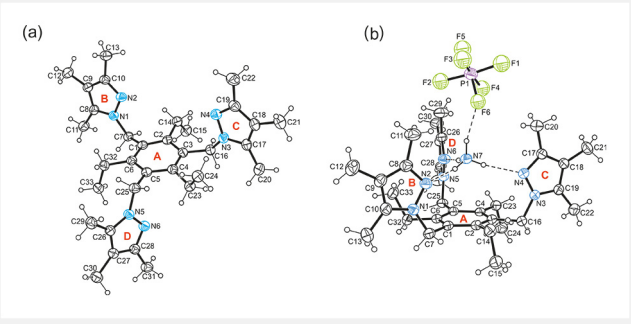

Figure 10 Perspective views (ORTEP diagrams) of **1** (a) and the ammonium complex in the crystal structure **1a** (b) including atom numbering and ring specification. The displacement ellipsoids are drawn at the 40% probability level. Dashed lines represent hydrogen bond interactions. In complex **1a**, only the major disorder component of the PF_6^- ion is shown for clarity.

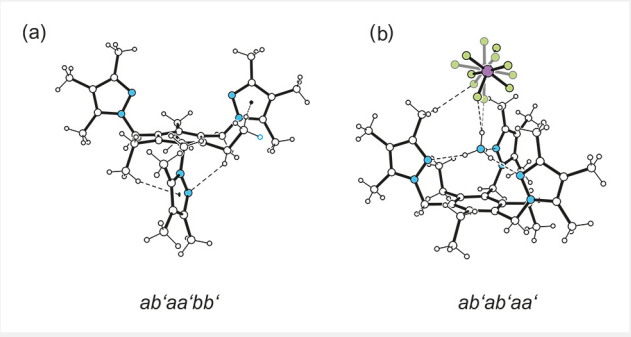

Figure 11 Ball-and-stick representations (side views) of **1** (a) and complex **1a** (b). Dashed lines represent hydrogen bond interactions.

be stabilized by two intramolecular C–H···π interactions[15] [*d*(H···*Cg*) 2.68, 2.77 Å] and one C–H···N bond[16] [*d*(H···N) 2.57 Å].

For steric reasons, the presence of the ethyl groups on the central arene ring prevents the formation of molecular dimers (as observed for trimethylbenzene-based derivative, see below). In the present crystal structure, the C–H···N bonds created by the atoms N(2), N(4), and N(6), as well as C–H···π contacts, provide a three-dimensional supramolecular architecture. A packing representation of **1** is given in Figure 12.

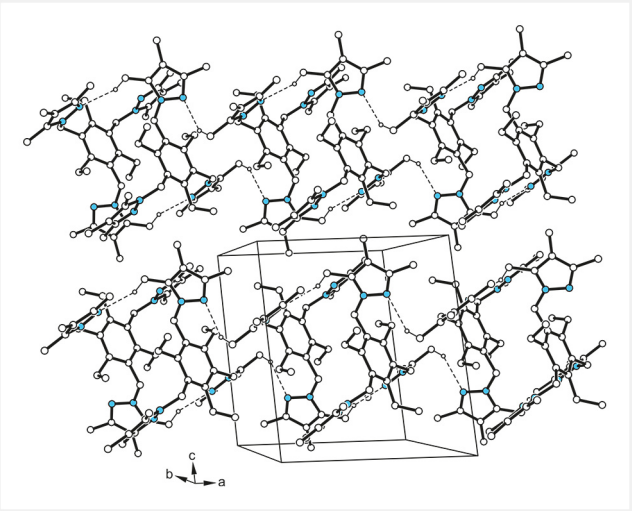

Figure 12 Packing diagram of **1**. Dashed lines represent hydrogen bond interactions.

Co-crystallization of receptor **1** and $NH_4^+PF_6^-$ from ethanol yields a complex of the structure displayed in Figures 10b and 11b, respectively. It should be noted here that the molecular structure of this complex is similar to those represented in published crystal structures of triethylbenzene-based receptors.[7a–d] The enhanced residual electron density near the PF_6^- ion indicates the presence of a O-H···F(P) bonded solvent molecule, which however could not be refined to an acceptable level. For this reason, a modified data set was generated using the SQUEEZE routine[17] of the PLATON program,[18] in which the contribution of the disordered molecule to the structural amplitudes was eliminated. A packing diagram of **1a** viewed down the *c*-axis is depicted in Figure 13.

The crystal structure of **2a** (space group $P2_1/c$) contains two independent but geometrically different complexes (Figure 14a). While the complex I adopts an *aa'aa'ab'* conformation, the substituents of the second complex follow an *aa'ab'ab'* arrangement (Figure 14b). The ethyl groups flanked by pyrazole rings are held in their positions by intramolecular C–H···π interactions [*d*(H···*Cg*) 2.50–2.79 Å]. The

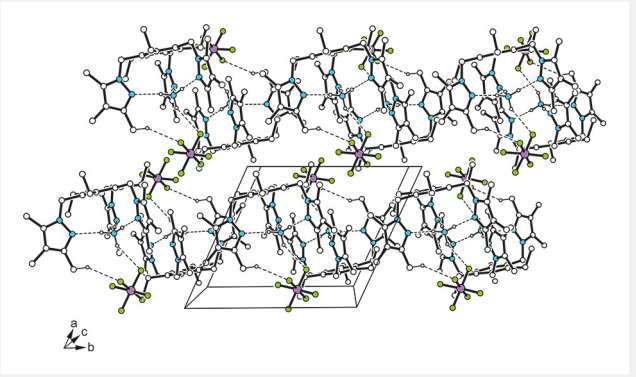

Figure 13 Packing diagram of **1a** viewed down the crystallographic *c*-axis. Dashed lines represent hydrogen bond interactions. Nitrogen atoms are displayed as blue, oxygens as red, fluorine as green and phosphorous atoms as violet circles.

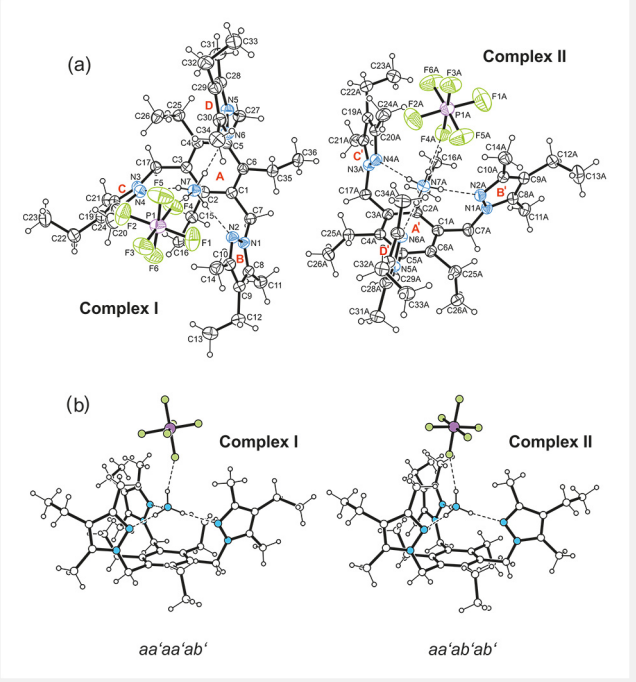

Figure 14 (a) Perspective view (ORTEP diagrams) of the molecular structure **2a** with atom labeling and specification of the aromatic rings. The displacement ellipsoids are drawn at the 40% probability level. (b) Ball-and-stick representations (side views) of the complexes in the crystal structure of **2a**. Dashed lines represent hydrogen bond interactions.

conformational differences between the receptor molecules are also reflected by the dihedral angles between their pyrazole rings, which are 67.3(1)°, 11.7(2)° and 66.5(1)° for complex I and 75.7(1)°, 47.8(1)° and 29.0(1)° for complex II.

Compared to **1a**, the modification of the receptor molecule by introducing an ethyl group in 4-position of the pyrazole rings exerts a significant influence on the packing behaviour of the molecules in the crystal (see Figure 15). Only one C–H···F bond[19] and one C–H···π interaction of each complex contribute to the molecular association, so that essentially van der Waals forces contribute to the stabilization of the crystal structure.

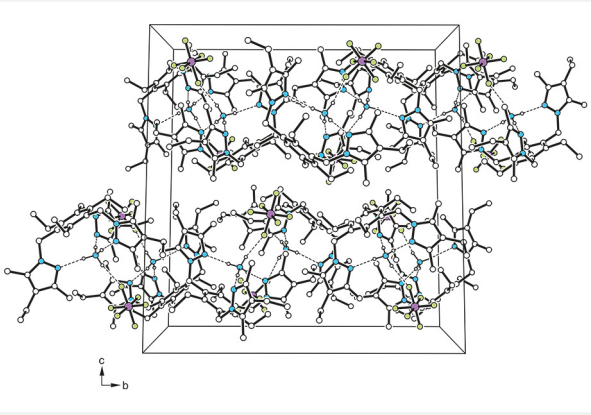

Figure 15 Packing diagram of **2a** viewed down the crystallographic *a*-axis. Dashed lines represent hydrogen bond interactions.

Trimethylbenzene-based compounds: Crystal structures of 3 and complexes 3a and 4a

Crystal growing of the compound **3** from methanol yields colourless blocks of the space group *P*-1 with one molecule in the asymmetric unit of the cell. In the solid state, the three pyrazole rings adopt, in the same fashion as in **1**, an *aab* arrangement (see Figure 16) with inclination angles of 79.9(1)°, 84.9(1)° and 86.0(1)° with respect to the plane of the benzene ring.

Figure 17 shows that the crystal structure is composed of dimers of closely nested molecules held together by C–H···N [*d*(H···N) 2.49–2.65 Å] and C–H···π interactions [*d*(H···*Cg*) 2.67 Å].

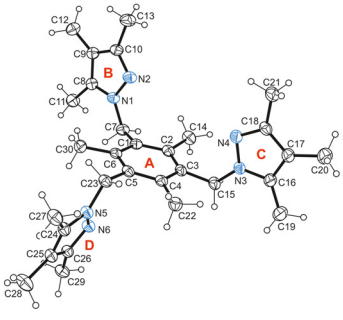

Figure 16 Perspective view (ORTEP plot) of the molecular structure of **3** including atom numbering and ring specification (A–D). The displacement ellipsoids are drawn at the 40% probability level.

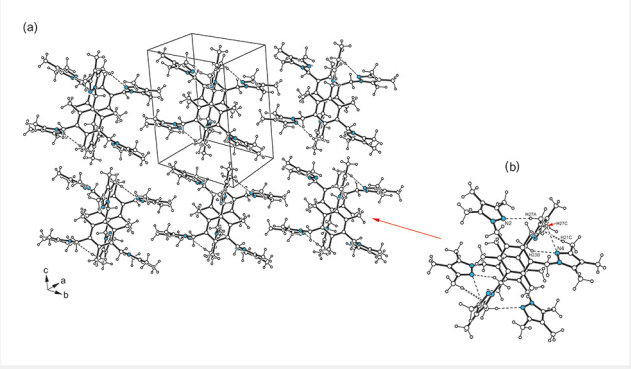

Figure 17 (a) Excerpt of the packing structure of **3**. (b) Structure of the molecular dimer including the labelling of coordinating atoms. Dashed lines represent hydrogen bond interactions and dashed double lines C–H···π contacts.

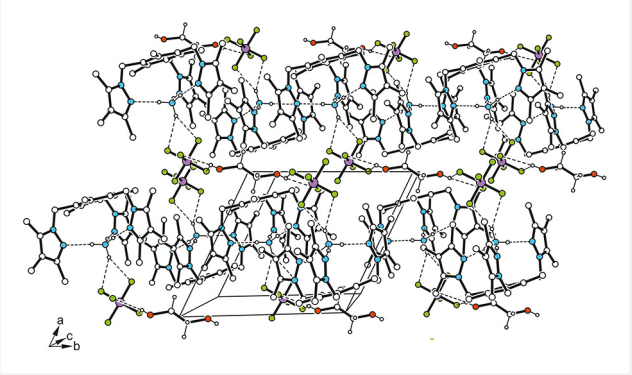

Figure 19 Packing diagram of **3a** viewed down the crystallographic c-axis. Dashed lines represent hydrogen bond interactions.

The colourless plate-like crystals of **3a** proved to be a solvate of the space group *P*-1 with the asymmetric part of the unit cell containing one complex unit **3**•$NH_4^+PF_6^-$ and one half of ethane-1,2-diol, i.e. the latter molecule is located on a crystallographic symmetry center. The structure of the complex is shown in Figure 18 In the crystal the receptor molecule exists in a symmetric conformation with an approximately coplanar arrangement (9.0°) of the pyrazole rings B and D. Within the receptor–NH_4^+ entity, N-H···N bond lengths are 2.03(5)–2.06(4) Å; the remaining hydrogen of NH_4^+ acts as a bifurcated binding site for formation of N-H···F bonds [*d*(H···F) 2.28(4), 2.51(4) Å] to the PF_6^- ion. The fluorine atoms F(3) and F(4) of this anion participate in the formation of O-H···F bonds [*d*(H···F) 2.45, 2.59 Å] to the solvent molecule.

The complexes are connected by C–H···F(P) type hydrogen bonds [*d*(H···F) 2.39–2.59 Å] and offset π···π interactions[20] [*d*(*Cg*···*Cg*) 3.928(1) Å, slippage 0.710 Å], the latter involving the pyrazole rings B and D. A comparative view of the packing structure of **3a** (Figure 19) and that of the ethyl-substituted analogous compound **1a** reveals only minor differences, which is also evident from the similarity of cell parameters.

Crystal growth of compound **4** in the presence of $NH_4^+PF_6^-$ yields colourless prism-like crystals of the space group *P*-1 with two receptor molecules, two $NH_4^+PF_6^-$ and two molecules of two-fold disordered ethanol in the asymmetric unit of the cell (complex **4a**). These components are connected to form two structurally similar complexes, as shown in Figure 20. Unlike **3a**, in the present case, no direct interactions between the NH_4^+ ion and its counter ion are observed. Instead, in each of the complexes, one H atom of the cation is associated to the oxygen atom of the alcohol molecule. The OH hydrogen of each solvent molecule is connected to the PF_6^- ion [*d*(H···F) 2.16(5)–2.50(4) Å].

C–H···F type hydrogen bonds [*d*(H···F) 2.55–2.61 Å] connect the complexes to a three-dimensional supramolecular

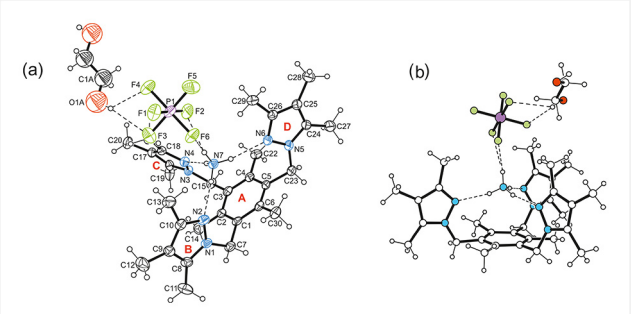

Figure 18 (a) Perspective view (ORTEP plot) of the molecular structure of complex **3a** including atom numbering and ring specification (A–D). The displacement ellipsoids are drawn at the 40% probability level. (b) Ball-and-stick representation (side view) of complex **3a**. Dashed lines represent hydrogen bond interactions.

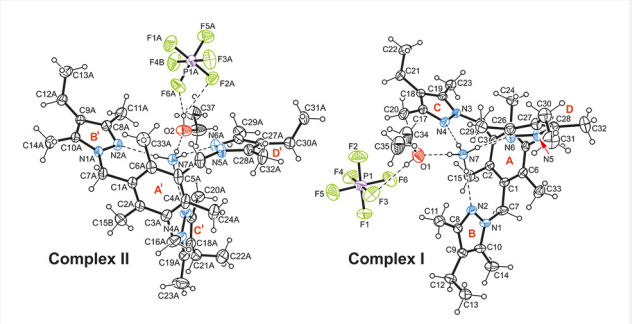

Figure 20 Perspective view (ORTEP plot) of the molecular structure of **4a** including atom numbering and ring specification (A–D). The displacement ellipsoids are drawn at the 30% probability level. For the sake of clarity, only one position of the disordered ethanol molecules is shown.

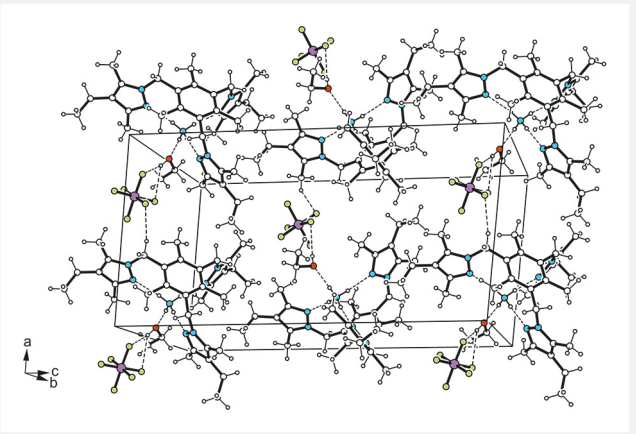

Figure 21 Packing diagram of **4a**. Dashed lines represent hydrogen bond interactions.

network. An excerpt of the packing structure of **4a** is displayed in Figure 21.

Conclusions

Representatives of the class of compounds consisting of a 1,3,5-trisubstituted 2,4,6-trialkylbenzene scaffold and bearing pyrazolyl groups are known to be able to act as ammonium receptors. The binding properties of these compounds towards NH_4^+ depend strongly on the substitution pattern of the pyrazole ring. In view of the promising properties of the derivatives bearing 3,5-dimethylpyrazolyl groups, the current studies investigated the extent to which the incorporation of an additional alkyl group in the 4-position of the pyrazole ring affects the binding properties of the new compounds **1**–**4**.

Binding studies revealed a two- to three-fold higher binding affinity of compounds **1**–**4**, bearing 3,4,5-trimethylpyrazolyl or 4-ethyl-3,5-dimethylpyrazolyl groups, compared to the analogues containing 3,5-dimethylpyrazolyl moieties. Particularly noteworthy is the improvement in the binding preference for NH_4^+ over K^+, which is clearly visible when considering the binding strength of compounds **1, 2** and **5** towards these two ions (for example, $K_{11}(NH_4^+)/K_{11}(K^+)$: 1 280 000 M^{-1}/119 M^{-1} vs. 451 000 M^{-1}/135 M^{-1} for **1** and **5**, respectively). Compounds consisting of the triethylbenzene scaffold and 3,4,5-trialkylpyrazole units were identified as the strongest receptors and found to have the best ability to discriminate between the two ions under the chosen experimental conditions. As expected, the strong solvent effects shown in previous binding studies with this type of receptors were also observed for the new compounds.

Crystalline complexes of compounds **1**–**4** with $NH_4^+PF_6^-$ were characterized by X-ray diffraction studies (crystal structures **1a**–**4a**). In each case, the pyrazolyl units of the receptor are directed towards the same face of the central benzene ring (*aaa* arrangement of the functionalized side arms) and interact with the ammonium ion via three NH···N hydrogen bonds. The molecular structures of these complexes are similar to those of the previously reported crystal structures of triethylbenzene- and trimethylbenzene-based receptors.[7a–d] However, it is remarkable that two of the four crystal structures (**2a** and **4a**) discussed in this work are characterized by the presence of two types of ammonium complexes. In the case of **2a**, for example, the difference between the two 1 : 1 complexes is related to different conformations of the receptor molecules; the arrangement of substituents around the benzene ring follows an *aa'aa'ab'* (complex I) and an *aa'ab'ab*' pattern (complex II). It is worth noting that the presence of two types of complexes was also observed by us for acyclic carbohydrate receptors in the crystal structures of complexes with glucopyranosides, which we have reported recently.[21] Among all crystalline complexes, direct contacts between NH_4^+ and PF_6^- (NH···F interactions) are observed for **1a**–**3a**, whereas solvent-mediated interactions between NH_4^+ and PF_6^- (NH···OH···F) are present in the ethanol-containing ammonium complex of the trimethylbenzene derivative **4**. The supramolecular motifs observed in the crystal structures of the free receptors and the ammonium complexes give valuable insights into the phenomena of molecular recognition processes.

Experimental Section

Analytical TLC was carried out on silica gel 60 F_{254} plates employing hexane/ethyl acetate, toluene/ethyl acetate or chloroform/methanol mixtures as the mobile phase. Flash chromatography was carried out on silica gel (for details, see below). Melting points are uncorrected. Compounds **5** and **6** were prepared via reactions of 1,3,5-tris(bromomethyl)-2,4,6-trimethylbenzene or 1,3,5-tris(bromomethyl)-2,4,6-triethylbenzene with 3,5-dimethyl-1*H*-pyrazole according to the procedure in refs. 7b, 22 and 23 (see also ref. 24).[7b,22–24]

Procedures

General procedure for the synthesis of compounds 1–4

To 3,4,5-trimethyl- or 4-ethyl-3,5-dimethyl-1*H*-pyrazole (4.5 equiv) dissolved under a N_2 atmosphere in anhydrous acetonitrile, sodium hydride (95%, 4.5 equiv) was added and the mixture was stirred for 30 minutes at room temperature. Then, 1,3,5-tris(bromomethyl)-2,4,6-triethylbenzene or 1,3,5-tris(bromomethyl)-2,4,6-trimethylbenzene (1.0 equiv) was added and the reaction mixture was stirred at room temperature under a N_2 atmosphere (the progress of

the reactions was monitored by thin layer chromatography). The reaction was quenched with H_2O (5 mL) and extracted with $CHCl_3$ (3 × 10 mL). The organic layers were combined, dried over Na_2SO_4 and filtered, and the solvent was removed under reduced pressure. The residue was purified by flash chromatography using hexane/ethyl acetate, toluene/ethyl acetate or chloroform/methanol as the eluent. The crude products were recrystallized from methanol, ethanol or hexane.

1,3,5-Tris[(3,4,5-trimethyl-1*H*-pyrazol-1-yl)methyl]-2,4,6-triethylbenzene (1)

The reaction of 1,3,5-tris(bromomethyl)-2,4,6-triethylbenzene (250 mg, 0.57 mmol) with 3,4,5-trimethyl-1*H*-pyrazole (281 mg, 2.55 mmol) and NaH (95%, 64 mg, 2.55 mmol) in CH_3CN (5 mL) afforded compound **1** as a white solid (flash chromatography: toluene/ethyl acetate, gradient 7 : 1–1 : 3, v/v; recrystallization from hexane).
Yield 190 mg (0.36 mmol, 63%).
R_f = 0.56 (hexane/ethyl acetate 1 : 1 v/v).
M. p. 171–172 °C.
^{1}H NMR ($CDCl_3$, 500 MHz): δ = 5.19 (s, 6 H), 2.76 (q, J = 7.5 Hz, 6 H), 2.09 (s, 9 H), 2.00 (s, 9 H), 1.86 (s, 9 H), 0.86 (t, J = 7.5 Hz, 9 H) ppm.
^{13}C NMR ($CDCl_3$, 125 MHz): δ = 145.9, 145.0, 136.0, 130.8, 111.6, 47.5, 23.8, 14.8, 12.0, 9.9, 8.2 ppm.
MS (ESI): *m/z* calcd for $C_{33}H_{48}N_6$ + H^+: 529.40 [M + H]$^+$; found: 529.47.
Elemental analysis calcd (%) for $C_{33}H_{48}N_6$: C, 74.96%; H, 9.15%; N, 15.89%. Found: C, 74.96%; H, 9.04%; N, 16.07%.

1,3,5-Tris[(3,4,5-trimethyl-1*H*-pyrazol-1-yl)methyl]-2,4,6-trimethylbenzene (3)

The reaction of 1,3,5-tris(bromomethyl)-2,4,6-trimethylbenzene (200 mg, 0.50 mmol) with 3,4,5-trimethyl-1*H*-pyrazole (249 mg, 2.26 mmol) and NaH (95%, 54 mg, 2.26 mmol) in CH_3CN (5 mL) afforded compound **3** as a white solid (flash chromatography: chloroform/methanol, gradient 50 : 1–7 : 1, v/v; recrystallization from methanol).
Yield 176 mg (0.36 mmol, 72%).
R_f = 0.72 (chloroform/methanol 16 : 1 v/v).
M. p. 246–247 °C.
^{1}H NMR ($CDCl_3$, 500 MHz): δ = 5.19 (s, 6 H), 2.23 (s, 9 H), 2.09 (s, 9 H), 1.98 (s, 9 H), 1.85 (s, 9 H) ppm.
^{13}C NMR ($CDCl_3$, 125 MHz): δ = 145.7, 138.1, 135.7, 131.4, 111.3, 48.7, 16.7, 12.0, 9.7, 8.1 ppm.
MS (ESI): *m/z* calcd for $C_{30}H_{42}N_6$ + H^+: 487.36 [M + H]$^+$; found: 487.39.
Elemental analysis calcd (%) for $C_{30}H_{42}N_6$: C, 74.03%; H, 8.70%; N, 17.27%. Found: C, 73.77%; H, 8.65%; N, 17.35%.

1,3,5-Tris[(4-ethyl-3,5-dimethyl-1*H*-pyrazol-1-yl)methyl]-2,4,6-triethylbenzene (2)

The reaction of 1,3,5-tris(bromomethyl)-2,4,6-triethylbenzene (250 mg, 0.57 mmol) with 4-ethyl-3,5-dimethyl-1*H*-pyrazole (317 mg, 2.55 mmol) and NaH (95%, 64 mg, 2.55 mmol) in CH_3CN (5 mL) afforded compound **2** as a white solid (flash chromatography: toluene/ethyl acetate, gradient 7 : 1–3 : 2, v/v, recrystallization from hexane).
Yield 210 mg (0.37 mmol, 65%).
R_f = 0.65 (toluene/ethyl acetate 1 : 1 v/v).
M. p. 171–172 °C.
^{1}H NMR (500 MHz, $CDCl_3$): δ = 5.19 (s, 6 H), 2.78 (q, J = 7.5 Hz, 6 H), 2.30 (q, J = 7.5 Hz, 6 H), 2.11 (s, 9 H), 2.02 (s, 9 H), 1.00 (t, J = 7.5 Hz, 9 H), 0.80 (t, J = 7.5 Hz, 9 H) ppm.
^{13}C NMR (125 MHz, $CDCl_3$): δ = 145.3, 144.9, 135.5, 130.9, 118.5, 47.4, 23.9, 16.8, 15.6, 14.6, 12.0, 9.7 ppm.
MS (ESI): *m/z* calcd for $C_{36}H_{54}N_6$ + H^+: 571.45 [M + H]$^+$; found: 571.49.
Elemental analysis calcd (%) for $C_{36}H_{54}N_6$: C, 75.74%; H, 9.53%; N 14.72%. Found: C, 75.67%; H, 9.48%; N 14.86%.

1,3,5-Tris[(4-ethyl-3,5-dimethyl-1*H*-pyrazol-1-yl)methyl]-2,4,6-trimethylbenzene (4)

The reaction of 1,3,5-tris(bromomethyl)-2,4,6-trimethylbenzene (300 mg, 0.75 mmol) with 4-ethyl-3,5-dimethyl-1*H*-pyrazole (420 mg, 3.38 mmol) and NaH (95%, 85 mg, 3.38 mmol) in CH_3CN (7 mL) afforded compound **4** as a white solid (flash chromatography: chloroform/methanol, gradient 99 : 1–13 : 1, v/v, recrystallization from ethanol).
Yield 303 mg (0.57 mmol, 76%).
R_f = 0.63 (chloroform/methanol 16 : 1 v/v).
M. p. 213–214 °C.
^{1}H NMR (500 MHz, $CDCl_3$): δ = 5.19 (s, 6 H), 2.29 (q, J = 7.5 Hz, 6 H), 2.22 (s, 9 H), 2.11 (s, 9 H), 1.98 (s, 9 H), 1.00 (t, J = 7.5 Hz, 9 H) ppm.
^{13}C NMR (125 MHz, $CDCl_3$): δ = 145.2, 138.0, 135.4, 131.6, 118.2, 48.8, 16.8 (2C), 15.6, 12.0, 9.6 ppm.
MS (ESI): *m/z* calcd for $C_{33}H_{48}N_6$ + H^+: 529.40 [M + H]$^+$; found: 529.47.
Elemental analysis calcd (%) for $C_{33}H_{48}N_6$: C, 74.96%; H, 9.15%; N 15.89%. Found: C, 74.79%; H, 9.10%; N, 15.78%.
The pyrazoles **9** and **10** were prepared according to the procedures in refs. 25 and 26 (see also ref. 27).[25–27] In addition to the purification methods described there, a dichloromethane solution of the crude reaction product was treated with a NaOH solution (2–5%).

Crystallographic data. The intensity data were collected at 123–213 K on a IPDS-2T diffractometer (Stoe & Cie, 2002) with MoK_α radiation (λ = 0.71 073 Å). Software for data collection and cell refinement: STOE X-AREA;[28] data reduction: X-RED.[28] Reflections were corrected for background, Lorentz and polarization effects. Preliminary structure models were derived by application of direct methods[29] and were refined by full-matrix least-squares calculation based on F^2

for all reflections.[30] With the exception of the disordered PF_6^- ion in **1a**, all non-hydrogen atoms were refined anisotropically. Apart from the OH hydrogen atoms in **4a**, all other H atoms were included in the models in calculated positions and were refined as constrained to bonding atoms. Crystallographic data for the structures in this paper have been deposited with the Cambridge Crystallographic Data Centre as supplementary publication numbers CCDC 2176612 (**1**), CCDC 2176613 (**1a**), CCDC 2176616 (**2a**), CCDC 2176614 (**3**), CCDC 2176615 (**3a**) and CCDC 2176617 (**4a**). Copies of the data can be obtained, free of charge, on application to CCDC, 12 Union Read, Cambridge CB2 1EZ, UK (Fax: +44-1223-336-033, Email: deposit@ccdc.cam.ac.uk).

Funding Information

F.F. thanks the Saxonian Ministry of Science, Culture and Tourism (SMWK) (project number 100327776) for his doctoral fellowship.

Open Access Funding by the Publication Fund of the Technische Universität Bergakademie Freiberg is gratefully acknowledged.

Supporting Information

Supporting Information for this article is available online at https://doi.org/10.1055/a-1896-6890.

Conflict of Interest

The authors declare no conflict of interest.

References

(1) (a) Ingildsen, P.; Olsson, G. *Water Sci. Technol.* **2002**, *46*, 139. (b) Kaelin, D.; Rieger, L.; Eugster, J.; Rottermann, K.; Bänninger, C.; Siegrist, H. *Water Sci. Technol.* **2008**, *58*, 629. (c) König, A.; Bachmann, T. T.; Metzger, J. W.; Schmid, R. D. *Appl. Microbiol. Biotechnol.* **1999**, *51*, 112. (d) Athavale, R.; Kokorite, I.; Dinkel, C.; Bakker, E.; Wehrli, B.; Crespo, G. A.; Brand, A. *Anal. Chem.* **2015**, *87*, 11990. (e) Reichert, J.; Sellien, W.; Ache, H. J. *Fresenius' J. Anal. Chem.* **1991**, *339*, 467. (f) Winkler, S.; Rieger, L.; Saracevic, E.; Pressl, A.; Gruber, G. *Water Sci. Technol.* **2004**, *50*, 105.

(2) (a) Zhang, W.; Zhang, J. PCT Int. Appl. WO2016/040048 A1, **2016**; (b) Radomska, A.; Bodenszac, E.; Głab, S.; Koncki, R. *Talanta* **2004**, *64*, 603. (c) Magalhães, J. M. C. S.; Machado, A. A. S. C. *Analyst* **2002**, *127*, 1069. (d) Wolfbeis, O. S.; Li, H. *Biosens. Bioelectron.* **1993**, *8*, 161. (e) Kovács, B.; Nagy, G.; Dombi, R.; Tóth, K. *Bionsens. Bioelectron.* **2003**, *18*, 111. (f) Kawabata, Y.; Sugamoto, H.; Imasaka, T. *Anal. Chim. Acta* **1993**, *283*, 689.

(3) (a) Sidey, V. *Acta Cryst.* **2016**, *B72*, 626. (b) Shannon, R. D. *Acta Cryst.* **1976**, *A32*, 751.

(4) (a) Siswanta, D.; Hisamoto, H.; Tohma, H.; Yamamoto, N.; Suzuki, K. *Chem. Lett.* **1994**, *23*, 945. (b) Bühlmann, P.; Pretsch, E.; Bakker, E. *Chem. Rev.* **1998**, *98*, 1593.

(5) (a) Suzuki, K.; Siswanta, D.; Otsuka, T.; Amano, T.; Ikeda, T.; Hisamoto, H.; Yoshihara, R.; Ohba, S. *Anal. Chem.* **2000**, *72*, 2200. (b) Sasaki, S.; Amano, T.; Monma, G.; Otsuka, T.; Iwasawa, N.; Citterio, D.; Hisamoto, H.; Suzuki, K. *Anal. Chem.* **2002**, *74*, 4845. (c) Graf, E.; Kintzinger, J. P.; Lehn, J. M.; LeMoigne, J. *J. Am. Chem. Soc.* **1982**, *104*, 1672. (d) Kim, H.-S.; Park, H. J.; Oh, H. J.; Koh, Y. K.; Choi, J.-H.; Lee, D.-H.; Cha, G. S.; Nam, H. *Anal. Chem.* **2000**, *72*, 4683. (e) Rahman, M. A.; Kwon, N.-H.; Won, M.-S.; Hyun, M.-H.; Shim, Y.-B. *Anal. Chem.* **2004**, *76*, 3660. (f) Jon, S. Y.; Kim, J.; Kim, M.; Park, S. H.; Jeon, W. S.; Heo, J.; Kim, K. *Angew. Chem. Int. Ed.* **2001**, *40*, 2116. (g) Campayo, L.; Pardo, M.; Cotillas, A.; Jaúregui, O.; Yunta, M. J.; Cano, C.; Gomez-Contreras, F.; Navarro, P.; Sanz, A. M. *Tetrahedron* **2004**, *60*, 979.

(6) Pazik, A.; Skwierawska, A. *Sens. Actuators, B* **2014**, *196*, 370.

(7) (a) Chin, J.; Walsdorff, C.; Stranix, B.; Oh, J.; Chung, H. J.; Park, S.-M.; Kim, K. *Angew. Chem. Int. Ed.* **1999**, *38*, 2756. (b) Chin, J.; Oh, J.; Jon, S. Y.; Park, S. H.; Walsdorff, C.; Stranix, B.; Ghoussoub, A.; Lee, S. J.; Chung, H. J.; Park S.-M.; Kim, K. *J. Am. Chem. Soc.* **2002**, *124*, 5374. (c) Koch, N.; Seichter, W.; Mazik, M.; *CrystEngComm* **2017**, *19*, 3817. (d) Schulze, M. M.; Koch, N.; Seichter, W.; Mazik, M. *Eur. J. Org. Chem.* **2018**, *2018*, 4317. (e) Jonah, T. M.; Mathivathanan, L.; Morozov, A. N.; Mebel, A. M.; Raptis, R. G.; Kavallieratos, K. *New J. Chem.* **2017**, *41*, 14835. (f) Rueda-Zubiaurre, A.; Herrero-García, N.; del Rosario Torres, M.; Fernández, I.; Osío Barcina, J. *Chem. Eur. J.* **2012**, *18*, 16884. (g) Ahn, K. H.; Kim, S.-G.; Jung, J.; Kim, K.-H.; Kim, J.; Chin, J.; Kim, K. *Chem. Lett.* **2000**, *29*, 170. (h) Kim, H.-S.; Kim, D.-H.; Kim, K. S.; Choi, J.-H.; Choi, H.-J.; Kim, S.-H.; Shim, J. H.; Cha, G. S.; Nam, H. *Talanta* **2007**, *71*, 1986. (i) Kim, H.-S.; Kim, D.-H.; Kim, K. S.; Choi, H.-J.; Shim, J. H.; Jeong, I. S.; Cha, G. S.; Nam, H. *J. Inclusion Phenom. Macrocyclic Chem.* **2003**, *46*, 201. (j) Oh, K. S.; Lee, C.-W.; Choi, H. S.; Lee, S. J.; Kim, K. S. *Org. Lett.* **2000**, *2*, 2679.

(8) (a) Koch, N.; Seichter, W.; Mazik, M. *Tetrahedron* **2015**, *71*, 8965. (b) Arunachalam, M.; Ahamed, B. N.; Ghosh, P. *Org. Lett.* **2010**, *12*, 2742.

(9) Fuhrmann, F.; Meier, E.; Seichter, W.; Mazik, M. *Acta Cryst.* **2022**, *E78*, doi: 10.1107/S2056989022006867.

(10) Hynes, M. J. *J. Chem. Soc., Dalton Trans.* **1993**, 311.

(11) Hübler, C. *Chem. – Methods* **2022**, e202200006, preprint; doi: 10.1002/cmtd.202200006.

(12) (a) Yoe, J. H.; Jones, A. L. *Ind. Eng. Chem. Anal. Ed.* **1944**, *16*, 111. (b) Meyer Jr., A. S.; Ayres, G. H. *J. Am. Chem. Soc.* **1957**, *79*, 49. (c) Chriswell, C. D.; Schilt, A. A. *Anal. Chem.* **1975**, *47*, 1623.

(13) (a) Hansch, C.; Leo, A.; Taft, R. W. *Chem. Rev.* **1991**, *91*, 165. (b) Taft, R. W. *J. Am. Chem. Soc.* **1952**, *74*, 2729. (c) Taft, R. W. *J. Am. Chem. Soc.* **1952**, *74*, 3120.

(14) Schulze, M.; Schwarzer, A.; Mazik, M. *CrystEngComm* **2017**, *19*, 4003.

(15) (a) Nishio, M. *Phys. Chem. Chem. Phys.* **2011**, *13*, 13873. (b) Nishio, M.; Umezawa, Y.; Honda, K.; Tsuboyama, S.; Suezawa, H. *CrystEngComm* **2009**, *11*, 1757. (c) Nishio, M.; Umezawa, Y.; Suezawa, H.; Tsuboyama S. In *The Importance of Pi-Interactions in Crystal Engineering: Frontiers in Crystal Engineering*; Tiekink, E. R. T.; Zukerman-Schpector, J., Eds.; Wiley: Hoboken, **2012**, 1.

(16) Desiraju, G. R.; Steiner, T. *The Weak Hydrogen Bond in Structural Chemistry and Biology*; Oxford University Press: Oxford, **1999**.

(17) Spek, A. L. *Acta Cryst.* **2015**, *C71*, 9.

(18) Spek, A. L. *Acta Cryst.* **2009**, *D65*, 148.

(19) Grepioni, F.; Cojazzi, G.; Draper, S. M.; Scully, N.; Braga, D. *Organometallics* **1998**, *17*, 296.
(20) (a) Dance, I. In *Encyclopedia of Supramolecular Chemistry*; Atwood, J. L.; Steed, J. M., Eds; Dekker: New York, **2004**, 1076. (b) James, S. L. In *Encyclopedia of Supramolecular Chemistry*, Vol. 1; Atwood, J. L.; Steed, J. M., Eds; Dekker: New York, **2004**, 1093. (c) Salonen, L. M.; Ellermann, M.; Diederich, F. *Angew. Chem. Int. Ed.* **2011**, *50*, 4808; *Angew. Chem.* **2011**, *123*, 4908.
(21) (a) Köhler, L.; Seichter, W.; Mazik, M. *Eur. J. Org. Chem.* **2020**, *2020*, 7023. (b) Köhler, L.; Hübler, C.; Seichter, W.; Mazik, M. *RSC Adv.* **2021**, *11*, 22221.
(22) Koch, N.; Mazik, M. *Synthesis* **2013**, *45*, 3341.
(23) Andree, S. N. L.; Sinha, A. S.; Aakeröy, C. B. *Molecules* **2018**, *23*, 163.
(24) Hartshorn, C. M.; Steel, P. J. *Aust. J. Chem.* **1995**, *48*, 1587.
(25) Morin, T. J.; Wanniarachchi, S.; Gwengo, C.; Makura, V.; Tatlock, H. M.; Lindeman, S. V.; Bennett, B.; Long, G. J.; Grandjean, F.; Gardinier, J. R. *Dalton Trans.* **2011**, *40*, 8024.
(26) Hillier, A. C.; Zhang, X. W.; Maunder, G. H.; Liu, S. Y.; Eberspacher, T. A.; Metz, M. V.; McDonald, R.; Domingos, A.; Marques, N.; Day, V. W.; Sella, A.; Takats, J. *Inorg. Chem.* **2001**, *40*, 5106.
(27) Ardizzoia, G.A.; Brenna, S.; Durini, S.; Therrien, B.; Trentin, I. *Dalton Trans.* **2013**, *42*, 12265.
(28) Stoe & Cie. *X-AREA* and *X-RED*. STOE & Cie GmbH: Darmstadt, Germany, **2009**.
(29) Sheldrick, G. M. *Acta Cryst.* **2015**, *A71*, 3.
(30) Sheldrick, G. M. *Acta Cryst.* **2015**, *C71*, 3.